Supplementary Information (SI) for Environmental Science: Water Research & Technology.
This journal is © The Royal Society of Chemistry 2026

Supplementary Materials

Characterizing the Impact of Geometry on the Performance of Inline-Coagulation Pretreatment Systems with Helical Flocculators

Joseph D. Ladouceur[a] , Roberto M. Narbaitz, PhD[a], Christopher Q. Lan, PhD[b]

[a] *Department of Civil Engineering, University of Ottawa, 161 Louis Pasteur Pvt., K1N 6N5, Ottawa, Canada*

[b] *Department of Chemical and Biological Engineering, University of Ottawa, 161 Louis Pasteur Pvt., K1N 6N5, Ottawa, Canada*

Corresponding Author E-mail: jlado088@uottawa.ca

Table of Contents

S.1. Additional Methodological Details

S.1.1. Preparation of Stock Model Organics

Bovine Serum Albumin (BSA) was found to be readily dissolvable in deionised water (DI). Accordingly, 0.5 g BSA was transferred to a half-full volumetric flask using a glass weighing scoop, the flask was swirled to dissolve the BSA and then brought to volume using DI. The stock solution of humic acid (HA) was prepared by initially dissolving 0.5 g of HA in 100 mL of 0.025 M NaOH using a 250 mL Erlenmeyer flask (Pyrex Conical Flask, Corning, NY) with vigorous mixing by magnetic stir bar as recommended by others.[1,2] Following several hours of stirring, the solution (and rinsate) was transferred to a 1 L volumetric flask (Lifetime-Red 5660 Class-A, Corning, NY) and brought to volume using DI. The sodium alginate (SA) solution was prepared by dissolving 0.5 g of the model organic initially into 250 mL of DI in a 400 mL griffin beaker (1000400, Corning, NY). As SA is difficult to completely dissolve, a variable speed mixer (OS-200D-C-SYS, Cole Parmer, Quebec, QC) set to 1,100 rpm was used to induce a vortex in the beaker prior to the addition of the powdered SA at a point near the impeller shaft. After vigorous mixing for at least 2 h, the solution (and rinsate) was transferred to a 1 L volumetric flask (Lifetime-Red 5660 Class-A, Corning, NY) and brought to volume. All stock solutions were magnetically stirred for a period of 24 h (VWR Advance Stirrer, VWR, Mississauga, ON, Canada) prior to being filtered through a 0.45 μm membrane (Supor 47 mm, 60043, Pall, NY) to remove residual insoluble matter. Filtered solutions were placed in sterilized (SR-24B, Consolidated Sterilizer Systems, Billerica, MA) glass 1 L volumetric flasks and stored in the dark at 4 °C prior to use. Stock solutions were stirred and brought to room temperature prior to the preparation of all working solutions.

S.1.2. Preparation of Synthetic Water

Synthetic water was prepared using the large baffled completely mixed reactor developed by Gonzalez-Galvis and Narbaitz.[3,4] Initially, the reactor, its baffle insert, and the impeller were rinsed thoroughly with distilled water (DW). The baffle insert and the impeller (10 cm x 10 cm stainless steel) were placed inside the reactor and the assembly placed on a high-resolution industrial balance (Model 3807MP8-1, Sartorius Gottingen, Germany). Then, the reactor was filled with a measured amount of DW which has been passed through a five-stage commercial reverse osmosis-activated carbon system (TGI-525 NO. 92821, TGI Pure Water Systems, Brea, CA). Pre-calculated volumes of stock model organic compounds were measured using mechanical pipettors (High Performance Pipettor, VWR, Mississauga, ON, Canada) and/or volumetric flasks (Class A, Corning, New York, NY) and added to the reactor.

Next, the inorganic background components including kaolin clay (~5 mg L^{-1}, corresponding to a turbidity of 5.5 NTU, Laboratory Grade 75185, Fisher Scientific, Hampton, NH), calcium chloride (0.6mM, Dried Powder 97%, Thermo Scientific, Hampton, NH), and sodium bicarbonate (0.9 mM, Certified ACS, Fisher Scientific, Hampton, NH) were added to the reactor and it was brought to the desired volume. The reactor was then inserted into its frame and the motor (Stir-Pak high torque, low-speed mixer 50007-12, Cole Parmer, Quebec, QC, Canada) put in place. The motor was set to its top speed (setting 10 on the speed controller, which is approximately a G value of 296 s^{-1}) to provide intense mixing of the contents of the reactor. The batches of synthetic water were thoroughly mixed in this system for a period of more than 2 h.

S.1.3. HRT Determination of Tested Helically Coiled Tube Flocculators (HCTFs)

The flowrate used in the majority of this study was 5 mL min^{-1}, which was selected to simulate conditions typical of bench-scale low-pressure membrane tests. A sample calculation estimating the mean hydraulic residence time (HRT) of the 1000 mm length HCTF with 3.175 mm pipe diameter is provided below.

$$holdup\ vol. = \frac{\pi L d^2}{4}$$

Where: L is the HCTF pipe length, cm

d is the HCTF pipe diameter, cm

$$holdup\ vol. = \frac{\pi(100\ cm)(0.3175\ cm)^2}{4} = 7.92\ cm^3$$

$$Residence\ Time = \frac{holdup\ vol.}{Flowrate}$$

$$Residence\ Time = \frac{7.92\ cm^3}{\frac{5\ mL}{min} \times \frac{cm^3}{mL}} \cong 1.6\ min$$

HRT values for other HCTF configurations operated at 5 mL min^{-1} are computed similarly and are presented in Table S1 below. Note for the full factorial design, only pipes of 3.175 mm were considered, while for the preliminary screening study pipe diameters of 4.7625 mm and 6.35 mm were also investigated.

Table S1. HRT Values for Different HCTF Geometries.

HRT (min)	Pipe Length (mm)		
Pipe Diameter (mm)	1000	1500	2000
3.175	1.60	2.4	3.2
4.7625	3.56	5.34	7.12
6.35	6.33	9.5	12.66

S.1.4. Jar Test Results for Challenge Water

To select a coagulant type for the synthetic water used in this study, preliminary jar testing was conducted using both aluminum- and iron-based coagulants. The tested coagulants were provided courtesy of Kemira Water Solutions Canada Inc. and include alum (ALS), polyaluminum chloride (PAX-XL8), ferric sulfate (PIX-312), aluminum chlorohydrate (PAX-XL1900), and alufer (ALS-3330). The ALS-3330 product contains a blend of ferric and aluminum sulfates at a mass ratio of 25% ferric to 75% aluminum. A summary of the principal characteristics of the different coagulants tested is provided in Table S2 below.

Table S2. Coagulant Technical Data

Product Name	Specific Gravity	Aluminum or Iron (%)	Basicity (%)
ALS	1.32	4.3	N/A
ALS-3330 (Alufer)	1.38	3-3.5 (Al) 2.4-3.6 (Fe)	N/A
PAX-XL8 (PACl)	1.2-1.28	5.2-5.8	65-75
PAX-XL1900 (ACH)	1.32-1.35	12.1-12.7	82.4-84.2
PIX-312 (Ferric Sulfate)	1.51-1.58	12-12.7	N/A

Several studies have noted that pre-coagulation using conditions that yield circumneutral zeta potential values is an effective strategy to reduce membrane fouling.[2,5] Accordingly, in this jar test study, the efficiency of each coagulant type with this synthetic water was assessed in terms of the zeta potential reduction. Samples of coagulated water were collected immediately following rapid mixing and analyzed for zeta potential using a zetasizer nano

particle analyzer (Nano ZS Series Model ZEN 3600, Malvern Instruments Ltd., Worcestershire, UK) with a folded capillary cell (DTS1060/1070, Malvern Instruments Ltd., Worcestershire, UK). The variation in zeta potential as a function of applied coagulant dose (reported as metal) is shown in Fig. S1.

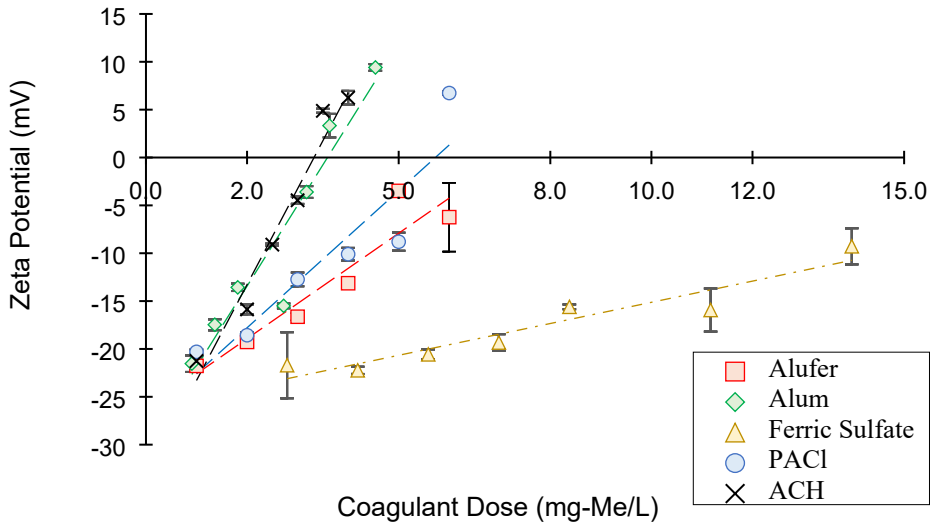

Fig. S1. Efficiency of alum compared to alternative coagulant types for synthetic challenge water.

As alum, which is a lower-cost coagulant, performed similarly to the pre-polymerized ACH coagulant, it was selected for further investigation. Additional jar testing was performed to identify the optimal conditions, in terms of dissolved organic carbon (DOC) removal, to use in the preliminary screening study. Fig. S2 below presents the removal of DOC as a function of the alum dose and coagulated pH, where it can be seen that the removals are maximized near a dose of 3 mg-Al L^{-1} and a pH of 6. The DOC removals were consistently high and exceeded that which would be expected for a natural water with a similar specific UV absorbance at 254 nm (SUVA) value,[6] indicating that this synthetic water is not fully representative of the behaviour of natural waters. This observation is consistent with the findings by Kim and Dempsey,[7] who reported important differences in the chemical composition and molecular weight distribution between natural waters and their surrogate organic compounds, which resulted in altered membrane fouling behaviour.

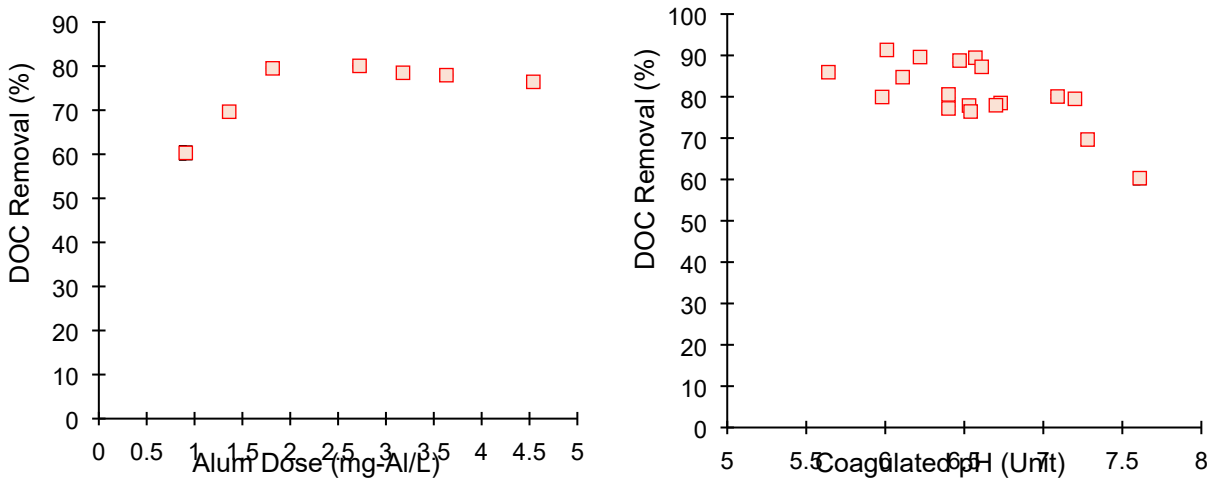

(a) **(b)**

Fig. S2. Removal of DOC by alum coagulant with varying: **(a)** Dose as aluminum; **(b)** Coagulated pH.

S.2. Preliminary Screening Study

As part of a sequential experimentation strategy, an unreplicated fractional factorial design of resolution IV was initially performed to screen among six different coagulation chemistry and HCTF geometry factors to identify which (if any) had the largest effects on the response variables, namely the floc equivalent circular diameter (ECD), floc concentration, and floc fractal dimension. The selection of a resolution IV design permits efficient estimation of the main effects of the six individual factors (using only 16 tests) as they are only confounded with three-factor or higher interactions, which are almost always negligible in magnitude. Those factors which had the greatest effect were subsequently investigated more thoroughly in the 2^3 full-factorial design.

S.2.1. Factorial Design and Alias Structure

A one quarter fraction of the general 2^k design, denoted as 2^{k-2}, can be constructed by first writing down the basic full-factorial design for $k-2$ factors and then adding two additional columns based on generators chosen from interactions involving the first $k-2$ factors.[8] The generators (words) for the one quarter fraction 2^{6-2}_{IV} screening design are $x_5 = x_1x_2x_3$ and $x_6 = x_2x_3x_4$. The defining relation for the design is the set of all columns which is equal to the identity matrix and can be determined using the generators:

$x_5 \cdot x_5 = x_1x_2x_3 \cdot x_5$

$I = x_1x_2x_3x_5$

Similarly, $I = x_2x_3x_4x_6$. From the product of the two generators, we also have the following:

$I = x_1x_2x_3x_5 \cdot x_2x_3x_4x_6$

$I = x_1x_4x_5x_6$

$\therefore I = x_1x_4x_5x_6 = x_1x_2x_3x_5 = x_2x_3x_4x_6$

It can be noted here that the resolution of the design (i.e., IV) is equal to the number of letters in the shortest word. As aforementioned, the design is constructed by first writing out the basic design for a full 2^4 two-level factorial design with 16 runs. The columns x_5 and x_6 are added in what is termed the calculation matrix by multiplying the

coded factor settings (i.e., high- and low-level factor settings) from the generator term. A sample calculation is provided below for the first row of x_5 in Table S3:

$x_5 = x_1x_2x_3$

$x_5 = (-1)(-1)(-1) = (-1)$

Table S3. Treatment Combinations for 2^{6-2}_{IV} Screening Design.

x_0	x_1	x_2	x_3	x_4	$x_5 = x_1x_2x_3$	$x_6 = x_2x_3x_4$	**Treatment**
(+1)	(–1)	(–1)	(–1)	(–1)	(–1)	(–1)	
(+1)	(+1)	(–1)	(–1)	(–1)	(+1)	(–1)	x_1x_5
(+1)	(–1)	(+1)	(–1)	(–1)	(+1)	(+1)	$x_2x_5x_6$
(+1)	(+1)	(+1)	(–1)	(–1)	(–1)	(+1)	$x_1x_2x_6$
(+1)	(–1)	(–1)	(+1)	(–1)	(+1)	(+1)	$x_2x_5x_6$
(+1)	(+1)	(–1)	(+1)	(–1)	(–1)	(+1)	$x_1x_3x_6$
(+1)	(–1)	(+1)	(+1)	(–1)	(–1)	(–1)	x_2x_3
(+1)	(+1)	(+1)	(+1)	(–1)	(+1)	(–1)	$x_1x_2x_3x_5$
(+1)	(–1)	(–1)	(–1)	(+1)	(–1)	(+1)	x_4x_6
(+1)	(+1)	(–1)	(–1)	(+1)	(+1)	(+1)	$x_1x_4x_5x_6$
(+1)	(–1)	(+1)	(–1)	(+1)	(+1)	(–1)	$x_2x_4x_5$
(+1)	(+1)	(+1)	(–1)	(+1)	(–1)	(–1)	$x_1x_2x_4$
(+1)	(–1)	(–1)	(+1)	(+1)	(+1)	(–1)	$x_3x_4x_5$
(+1)	(+1)	(–1)	(+1)	(+1)	(–1)	(–1)	$x_1x_3x_4$
(+1)	(–1)	(+1)	(+1)	(+1)	(–1)	(+1)	$x_2x_3x_4x_6$
(+1)	(+1)	(+1)	(+1)	(+1)	(+1)	(+1)	$x_1x_2x_3x_4x_5x_6$

It should be noted that the treatment combinations presented in Table S3 are in standard order, which differs from the randomized order that the experiments were conducted to eliminate the possibility for interferences by unknown systematic or happenstance errors.

The alias or confounding pattern of the design can be obtained by multiplying the effects by each word of the defining relation. A sample calculation is shown below for first, second, and third order effects while a summary of all the aliasing relationships is presented in Table S4.

For the Main Effect x_1:

$I = x_1x_2x_3x_5 = x_2x_3x_4x_6 = x_1x_4x_5x_6$

$x_1 \cdot I = x_1 \cdot x_1x_2x_3x_5 = x_1 \cdot x_2x_3x_4x_6 = x_1 \cdot x_1x_4x_5x_6$

$x_1 = x_2x_3x_5 = x_1x_2x_3x_4x_6 = x_4x_5x_6$

For the Interaction Effect x_1x_2:

$I = x_1x_2x_3x_5 = x_2x_3x_4x_6 = x_1x_4x_5x_6$

$x_1x_2 \cdot I = x_1x_2 \cdot x_1x_2x_3x_5 = x_1x_2 \cdot x_2x_3x_4x_6 = x_1x_2 \cdot x_1x_4x_5x_6$

$x_1x_2 = x_3x_5 = x_1x_3x_4x_6 = x_2x_4x_5x_6$

For the Interaction Effect $x_1x_2x_3$:

$I = x_1x_2x_3x_5 = x_2x_3x_4x_6 = x_1x_4x_5x_6$

$x_1x_2x_3 \cdot I = x_1x_2x_3 \cdot x_1x_2x_3x_5 = x_1x_2x_3 \cdot x_2x_3x_4x_6 = x_1x_2x_3 \cdot x_1x_4x_5x_6$

$x_1x_2x_3 = x_5 = x_1x_4x_6 = x_2x_3x_4x_5x_6$

Table S4. Alias Structure for Screening Design

Main Effects	Two Factor Interactions
$x_1 = x_2x_3x_5 = x_1x_2x_3x_4x_6 = x_4x_5x_6$	$x_1x_2 = x_3x_5 = x_1x_3x_4x_6 = x_2x_4x_5x_6$
$x_2 = x_1x_3x_5 = x_3x_4x_6 = x_1x_2x_4x_5x_6$	$x_1x_3 = x_2x_5 = x_1x_2x_4x_6 = x_3x_4x_5x_6$
$x_3 = x_1x_2x_5 = x_2x_4x_6 = x_1x_3x_4x_5x_6$	$x_1x_4 = x_5x_6 = x_2x_3x_4x_5 = x_1x_2x_3x_6$
$x_4 = x_2x_3x_6 = x_1x_5x_6 = x_1x_2x_3x_4x_5$	$x_1x_5 = x_2x_3 = x_4x_6 = x_1x_2x_3x_4x_5x_6$
$x_5 = x_1x_2x_3 = x_1x_4x_6 = x_2x_3x_4x_5x_6$	$x_1x_6 = x_4x_5 = x_2x_3x_5x_6 = x_1x_2x_3x_4$
$x_6 = x_2x_3x_4 = x_1x_4x_5 = x_1x_2x_3x_5x_6$	$x_2x_4 = x_3x_6 = x_1x_3x_4x_5 = x_1x_2x_5x_6$
	$x_2x_6 = x_3x_4 = x_1x_3x_5x_6 = x_1x_2x_4x_5$
Three Factor Interactions	
$x_1x_2x_4 = x_3x_4x_5 = x_1x_3x_6 = x_2x_5x_6$	$x_1x_3x_4 = x_2x_4x_5 = x_1x_2x_6 = x_3x_5x_6$

S.2.2. Experimental Factors for Screening Design

The selection of factor settings for the HCTF geometrical parameters was already described in the manuscript. Measures of coagulation chemistry, including the coagulant dose (x_1) and coagulated pH (x_6), were also considered as factors due to the strong influence they are known to exert on properties of the formed flocs.[9,10] The high factor setting of the coagulant dose was set to the optimum for DOC removal based on the results of preliminary jar testing (see Section S.1.4), while the low factor setting was specified as a 20% reduced dose, which has been reported by some

authors to lead to the lowest permeability decline in inline coagulation pretreatment systems.[11] The high and low factor settings for coagulation pH were selected based on the aluminum coagulation domain presented by Amirtharajah and Mills[12] as well as the humic and fulvic acid removal domains presented by Edwards and Amirtharajah[13] and Hundt and O'Melia,[14] respectively. A summary of the factor settings for the preliminary screening study is presented in Table S5.

Table S5. Controlled Factor Level Settings for Preliminary Screening Design

		Levels	
Factors	**Unit**	**(-1)**	**(+1)**
x_1: Coagulant Dose	mg-Al L^{-1}	2.4	3
x_2: Coil Pitch	(mm)	15	45
x_3: Pipe Length	(mm)	1000	2000
x_4: Coil Diameter	(mm)	50	100
x_5: Pipe Diameter	(mm)	3.175 (1/8")	6.35 (1/4")
x_6: Coagulation pH	Unit	6	7

S.2.3. Results of Preliminary Screening Study

Table S6 - Table S8 below present the results of the screening study. Statistical analysis was performed using JMP® Pro 18 software (SAS Institute Inc., Cary, NC). Because the screening study is an unreplicated design, the software uses the method proposed by Lenth[15] where the t-statistic for the students t-test is calculated by dividing the parameter estimate by the Lenth pseudo-standard error (PSE). A students t-test is then performed to determine the "pseudo" *p*-value for the parameter effect, with a threshold *p*-value ~0.2-0.25 considered for factor screening. The calculation of the Lenth PSE was performed according to Montgomery[16]. From Table S6 below, no effects were significant according to the criteria set out by JMP (i.e., $p > 0.25$), however, the coagulant dose and pH were found to have the greatest effect on ECD as they had the smallest *p*-values.

Table S6. Factor Screening Results for ECD

Parameter	**Estimate**	**Pseudo t-Ratio**	***p*-Value**
Intercept	44.4869	14.7014	<.0001
x_1: Dose	3.3692	1.1134	0.3162
x_2: Pitch	1.8138	0.5994	0.575
x_3: Length	-2.001	-0.6612	0.5377

x_4: Coil Diameter	2.2043	0.7284	0.499
x_5: Pipe Diameter	-2.0959	-0.6926	0.5194
x_6: pH	-3.5957	-1.1882	0.2881
Dose*Pitch	-0.8378	-0.2769	0.793
Dose*Length	1.8887	0.6242	0.5599
Dose*Coil Diameter	2.0174	0.6667	0.5345
Dose*Pipe Diameter	-2.9306	-0.9685	0.3773
Dose*pH	-1.3507	-0.4464	0.674
Pitch*Coil Diameter	-3.1201	-1.0311	0.3498
Pitch*pH	2.1401	0.7072	0.511
Dose*Pitch*Coil Diameter	-1.9266	-0.6367	0.5523
Dose*Length*Coil Diameter	-0.9266	-0.3062	0.7718

In Table S7, the pipe length and the interaction between the coagulant dose and coil pitch were found to have the most significant effects on the floc D_p, (i.e., $p < 0.2$).

Table S7. Factor Screening Results for D_p

Parameter	Estimate	Pseudo t-Ratio	*p*-Value
Intercept	1.6139	361.9101	<.0001
x_1: Dose	-0.00332	-0.7453	0.4896
x_2: Pitch	-0.00122	-0.273	0.7958
x_3: Length	0.00741	1.6614	0.1575
x_4: Coil Diameter	0.00564	1.2658	0.2614
x_5: Pipe Diameter	0.00086	0.1926	0.8548
x_6: pH	0.00265	0.5932	0.5789
Dose*Pitch	0.00724	1.6243	0.1652
Dose*Length	-0.00297	-0.6667	0.5345
Dose*Coil Diameter	0.00623	1.3976	0.2211
Dose*Pipe Diameter	-0.0026	-0.5836	0.5848
Dose*pH	0.0016	0.3584	0.7347
Pitch*Coil Diameter	0.00356	0.7981	0.461
Pitch*pH	-0.00537	-1.2033	0.2827
Dose*Pitch*Coil Diameter	0.00059	0.1327	0.8996
Dose*Length*Coil Diameter	-0.00244	-0.5464	0.6083

From Table S8, the effects of the coil pitch, the pH, as well as the interaction between the coagulant dose and coil diameter were found to have the greatest significance on the floc concentration (i.e., $p < 0.25$).

Table S8. Factor Screening Results for Floc Concentration

Parameter	Estimate	Pseudo t-Ratio	*p*-Value
Intercept	16451.7	10.6645	0.0001

x_1: Dose	153.7	0.0997	0.9245
x_2: Pitch	-2221.2	-1.4398	0.2095
x_3: Length	-773.2	-0.5012	0.6375
x_4: Coil Diameter	1049.6	0.6804	0.5265
x_5: Pipe Diameter	1588.7	1.0298	0.3503
x_6: pH	-3189.4	-2.0675	0.0935
Dose*Pitch	161.6	0.1048	0.9206
Dose*Length	-783.6	-0.5079	0.6331
Dose*Coil Diameter	-2153.8	-1.3961	0.2215
Dose*Pipe Diameter	588.3	0.3814	0.7186
Dose*pH	1177.3	0.7632	0.4798
Pitch*Coil Diameter	1028.4	0.6667	0.5345
Pitch*pH	1412.8	0.9158	0.4018
Dose*Pitch*Coil Diameter	546.6	0.3543	0.7376
Dose*Length*Coil Diameter	-105.4	-0.0683	0.9482

S.3. Estimation of Mean Velocity Gradient for Inline Static Mixer (ISM)

Due to privacy concerns related to product competitiveness, the manufacturer of the ISM does not make any data or formulas for calculating mixing quality/efficiency openly available. As a result, the mean velocity gradient (G) was estimated using Eq. S1 below: [17]

$$G = \sqrt{\frac{\rho g h}{\mu \tau}} \tag{S1}$$

where G is the mean velocity gradient (s^{-1}), h is the measured headloss across the mixer (m), μ is the dynamic viscosity of the solution, which for dilute streams at 20 °C is approximately $1.002 \times 10^{-3} \frac{kg}{m \cdot s}$, and τ is the hydraulic detention time (s). The headloss across the mixer can be expressed in terms of the pressure differential, which simplifies the expression to:

$$G = \sqrt{\frac{\Delta P}{\mu \tau}} \tag{S2}$$

Where ΔP is the measured pressure differential across the mixer (Pa) and all other terms have already been defined. In this study, the pressure differential across the mixer was evaluated by fitting a pair of pressure transducers (PX309-030AV, Omega Sensing Solution, St. Eustache, QC) to the mixer inlet and outlet in the bench-scale system. A LabView program (National Instruments, Austin, TX) was developed to automatically log the pressure readings from each location and calculate the differential pressure value. For the flowrate of 5 mL min^{-1}, the average pressure differential across the ISM was found to be 103.42 Pa and the HRT was estimated to be 2.58 min. The HRT estimation was based on a gravimetric approach: the ISM was filled with DI, the mass of which was subsequently measured using an analytical balance (AJ150, Mettler Toledo, Columbus, OH). Using the temperature corrected density, the volume of DI was determined, and the mean HRT was calculated by dividing the storage volume by the system flowrate. Therefore:

$$G = \sqrt{\frac{103.42 \frac{kg}{m \cdot s^2}}{1.002 \times 10^{-3} \frac{kg}{m \cdot s} \times 2.58\, min \times 60 s/min}}$$

$$G = 25.8\, s^{-1}$$

S.4. Additional Data for Full Factorial Design (FFD)

S.4.1. Randomized Run Order

To mitigate the risk of systematic bias or time-dependent trends in the results, the experiments for the full factorial design were carried out in a randomized order defined by Table S9.

Table S9. Randomized Run Order for 2^3 Full-Factorial Design

Pattern	Coil Diameter (mm)	Pipe Length (mm)	Coil Pitch (mm)
+ − +	75	1000	45
− + +	50	2000	45
+ + −	75	2000	15
0 0 0	62.5	1500	30
− − +	50	1000	45
− + −	50	2000	15
+ − −	75	1000	15
0 0 0	62.5	1500	30
+ + −	75	2000	15
+ − +	75	1000	45
− + +	50	2000	45
− − +	50	1000	45
+ + +	75	2000	45
0 0 0	62.5	1500	30
0 0 0	62.5	1500	30
− + −	50	2000	15
+ − −	75	1000	15
− − −	50	1000	15
0 0 0	62.5	1500	30
0 0 0	62.5	1500	30
+ + +	75	2000	45
− − −	50	1000	15

S.4.2. FFD Model Fitting and Adequacy Check

For a simple linear regression model, the errors at each value of the predictor should be normally distributed. Fig. S3 shows the normal quantile plot of residuals, which plots the observed residual quantiles against a theoretical normal quantile distribution. If the variable is normally distributed, the normal quantile plot approximates a diagonal straight line. The graphs in Fig. S3 show that the three response variables were normally distributed.

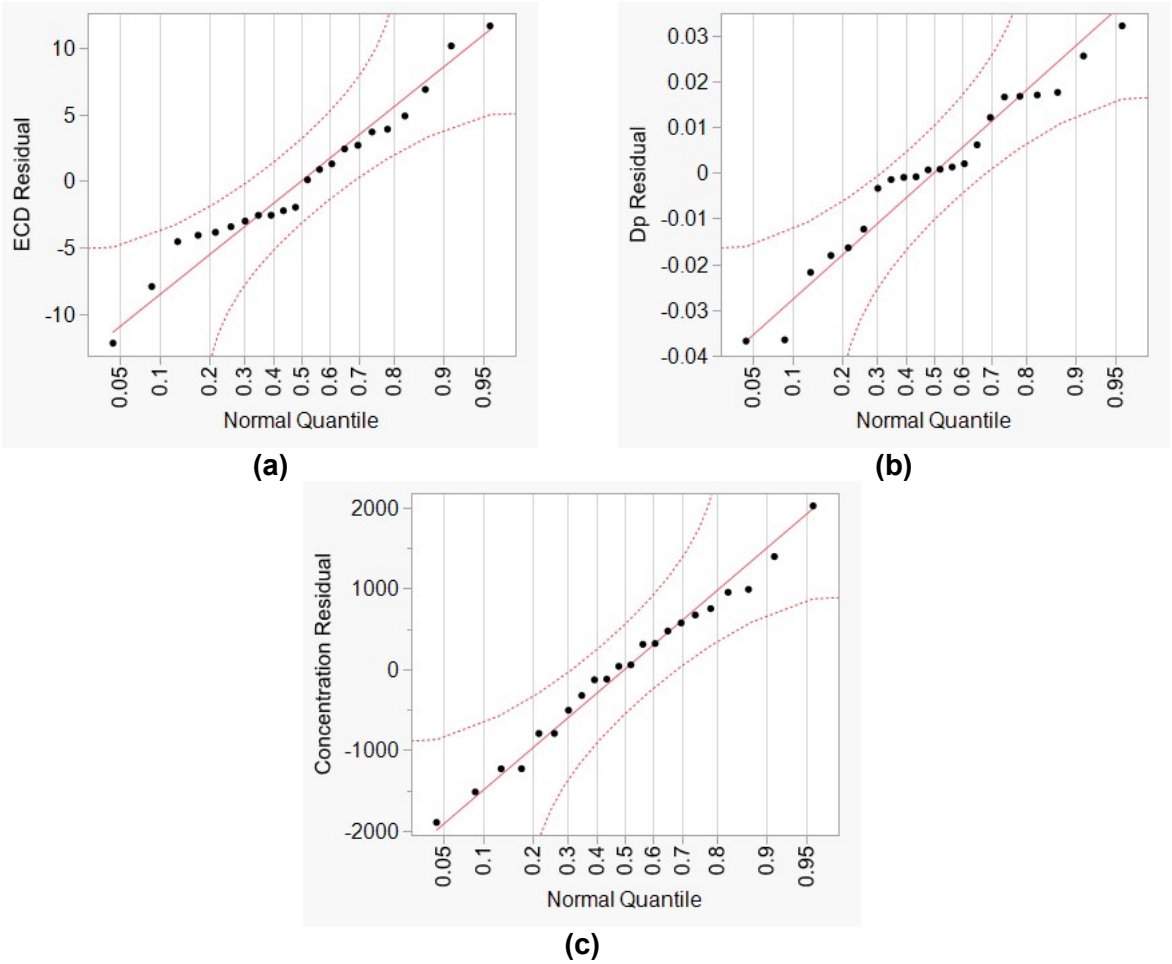

Fig. S3. QQ plots for model residuals: **(a)** ECD; **(b)** D_p; **(c)** Concentration

S.4.3 Test for Model Curvature in FFD

To test for curvature, a t-test (assuming unequal variances) was performed comparing the mean of the replicated center points to the mean of the replicated corner points as proposed by Montgomery[16].

The hypotheses are given by:

H_0:$\mu_{Center} = \mu_{Corner}$

H_1:$\mu_{Center} \neq \mu_{Corner}$

And the test statistic is given by:

$$t_0 = \frac{\bar{y_{Center}} - \bar{y_{Corner}}}{\sqrt{\frac{S_{Center}^2}{n_{center}} + \frac{S_{Corner}^2}{n_{corner}}}}$$

Using this approach, the test statistic and corresponding *p*-values can be computed for the three response variables considered in this study, namely, the ECD, D_p, and the floc concentration.

Table S10. Students t-Test for Assessment of Response Function Curvature

Response Variable	$\bar{y}_{Center} - \bar{y}_{Corner}$	t_0	***p*-value**
ECD	4.956	1.175886	0.2548
D_p	-0.01831	-1.5938	0.1284
Concentration	-1278.8	-1.4440	0.1659

Therefore, based on a significance level α=0.05, there is insufficient evidence ($p > 0.05$) to reject the null hypothesis for all three response variables. This finding suggests that the assumption of linearity by the factorial design holds and the first-order interaction model is adequate for modeling the factor effects.

S.4.4. Interaction Diagrams

As part of the analysis of the full factorial design results, this section provides the interaction diagrams for select parameters and response variables. From Fig. S4 below, the effect of coil pitch on ECD is seen to change depending on the setting of pipe length. For the short length HCTF, increasing coil pitch led to larger sized flocs whereas for the longer HCTF the floc size decreased with increasing coil pitch.

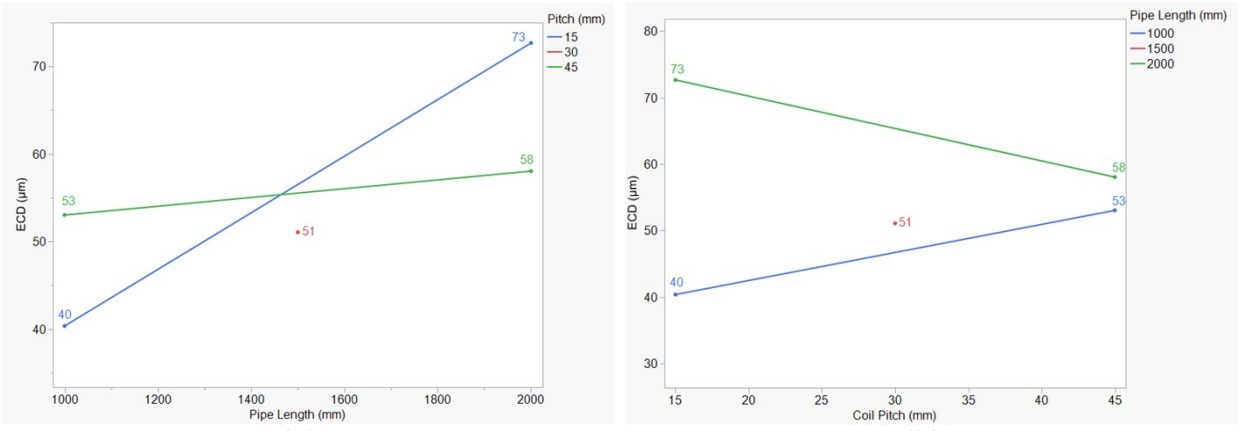

Fig. S4. Interaction diagrams between pipe length and coil pitch for floc ECD: **(a)** Effect of pipe length at high and low factor setting of coil pitch; **(b)** Effect of coil pitch at high and low factor settings of pipe length

At the high factor setting for coil pitch, the effect of increasing coil diameter leads to a more rapid decline in floc concentration compared to at the low factor setting (Fig. 5a). From Fig. S5b, the effect of coil pitch is changed depending on the setting of coil diameter. For HCTFs with large diameter, increasing the coil pitch reduced the floc concentration while for small diameter HCTFs the floc concentration increased slightly with increasing coil pitch. From Fig. S6 below, the effect of pipe length on floc concentration is greater at the low setting of coil diameter than for the large diameter HCTF. The effect of coil diameter on concentration is also seen to be greater for the short length HCTF compared to for the 2000 mm length flocculator.

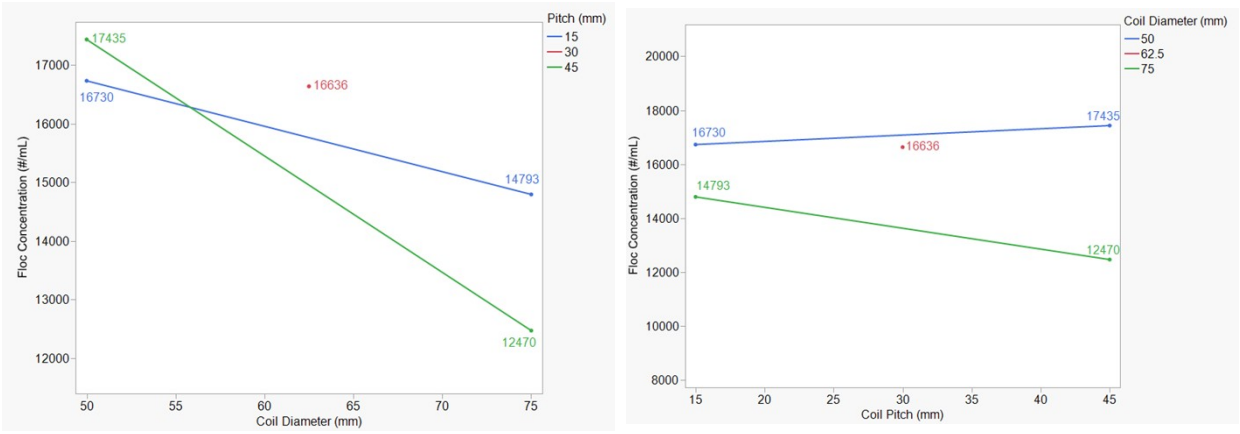

(a) **(b)**

Fig. S5. Interaction diagrams between coil diameter and coil pitch for floc concentration: **(a)** Effect of coil diameter at high and low factor setting of coil pitch; **(b)** Effect of coil pitch at high and low factor settings of coil diameter

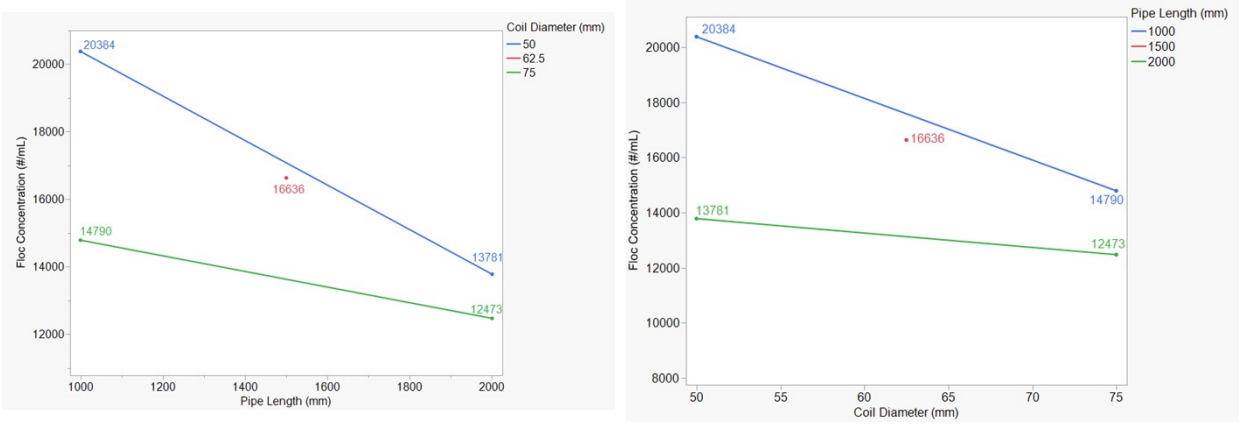

(a) **(b)**

Fig. S6. Interaction diagrams between coil diameter and pipe length for floc concentration: **(a)** Effect of pipe length at high and low factor setting of coil diameter; **(b)** Effect of coil diameter at high and low settings of pipe length

S.5.Correlation Analysis

This section presents the complete results of the multivariate correlation analysis between the three response variables (floc ECD, D_p, and floc concentration) and measures of floc curvature and torsion. Here, Eq. (S3) and Eq. (S4) were considered in addition to Eqs. (2) – (8), which were already presented in the manuscript.

$$\tau_{nd} = \frac{r_p b}{b^2 + r_c^2} \tag{S3}$$

$$\tau = \frac{p}{(r_c^2 + p^2)} \tag{S4}$$

Where τ_{nd} is the dimensionless torsion, τ is the torsion (mm^{-1}), b is the pitch slope ($mm\ rad^{-1}$), p is the coil pitch (mm), r_p is the pipe radius (mm), and r_c is the coil radius (mm). Tables S11 and S12 below present the regression results separated according to the factor setting for the pipe length. Below the diagonal the Pearson Correlation Coefficient values are presented while above the diagonal, shaded in grey, the *p*-values for the correlation are provided. Those shown to be significant with greater than 95% confidence are highlighted in red text.

Table S11. Multivariate Correlation Analysis Between Floc Response Variables and Measures of Torsion and Curvature for 1000 mm Pipe Length

L=1000	ECD (μm)	D_p	Conc. (#/mL)	De	δ_{nd}	τ_{nd}	λ	β_0	c	τ	γ
ECD (μm)		0.0203	0.7229	0.6630	0.6557	0.3157	0.1570	0.0922	0.7965	0.9240	0.1570
D_p	-0.9797		0.8508	0.7772	0.7682	0.2353	0.1230	0.0894	0.9158	0.8775	0.1230
Conc. (#/mL)	-0.2771	0.1492		0.0051	0.0064	0.4890	0.7267	0.8859	0.0046	0.1568	0.7267
De	-0.3370	0.2228	0.9949		<.0001	0.5472	0.7810	0.9352	0.0098	0.1482	0.7810
δ_{nd}	-0.3443	0.2318	0.9936	0.9999		0.5548	0.7879	0.9414	0.0112	0.1477	0.7879
τ_{nd}	0.6843	-0.7647	0.5110	0.4528	0.4452		0.0394	0.1030	0.4272	0.2961	0.0394
λ	0.8430	-0.877	0.2733	0.2190	0.2121	0.9606		0.0155	0.6497	0.4163	
β_0	0.9078	-0.9106	0.1141	0.0648	0.0586	0.8970	0.9845		0.8023	0.5128	0.0155
c	-0.2035	0.0842	0.9954	0.9902	0.9888	0.5728	0.3503	0.1977		0.1107	0.6497
τ	0.0760	-0.1225	0.8432	0.8518	0.8523	0.7039	0.5837	0.4872	0.8893		0.4163
γ	0.8430	-0.8770	0.2733	0.2190	0.2121	0.9606		0.9845	0.3503	0.5837	

Note: *p*-values are shown above the diagonal in shaded grey while Pearson correlation coefficients are shown below the diagonal in white; Correlations with significance at greater than 95% confidence are highlighted in red text.

Table S12. Multivariate Correlation Analysis Between Floc Response Variables and Measures of Torsion and Curvature for 2000 mm Pipe Length

L=2000	ECD (μm)	D_p	Conc. (#/mL)	De	δ_{nd}	τ_{nd}	λ	β_0	c	τ	γ
ECD (μm)		0.4827	0.8030	0.7150	0.7239	0.0193	0.0255	0.0694	0.5837	0.4467	0.0255
D_p	-0.5173		0.6814	0.0362	0.0379	0.3325	0.5300	0.6717	0.0101	0.0627	0.5300
Conc. (#/mL)	-0.1970	0.3186		0.6139	0.6226	0.8123	0.9728	0.8354	0.6062	0.9803	0.9728
De	-0.2850	0.9638	0.3861		<.0001	0.5472	0.7810	0.9352	0.0098	0.1483	0.7810
δ_{nd}	-0.2761	0.9621	0.3774	0.9999		0.5548	0.7879	0.9414	0.0112	0.1477	0.7879
τ_{nd}	-0.9807	0.6675	0.1877	0.4528	0.4452		0.0394	0.1030	0.4272	0.2961	0.0394
λ	-0.9745	0.4700	-0.0272	0.2190	0.2121	0.9606		0.0155	0.6497	0.4163	
β_0	-0.9306	0.3284	-0.1646	0.0648	0.0586	0.8970	0.9845		0.8023	0.5128	0.0155
c	-0.4163	0.9899	0.3938	0.9902	0.9888	0.5728	0.3503	0.1977		0.1107	0.6497
τ	-0.5533	0.9373	-0.0197	0.8518	0.8523	0.7039	0.5837	0.4872	0.8893		0.4163
γ	-0.9745	0.4700	-0.0272	0.2190	0.2121	0.9606		0.9845	0.3503	0.5837	

Note: *p*-values are shown above the diagonal in shaded grey while Pearson correlation coefficients are shown below the diagonal in white; Correlations with significance at greater than 95% confidence are highlighted in red text.

S.6. Batch Mixing Data

To prevent flocs from settling, the batch reactor mixing strategy involved continuous mixing at G-values higher than those used in conventional flocculation practice. Accordingly, to verify whether this caused a time-dependent effect on floc properties, samples of flocs were collected over the course of 3 hours after the addition of coagulant. The sample ECD and floc concentration are summarized in Fig. S7 below.

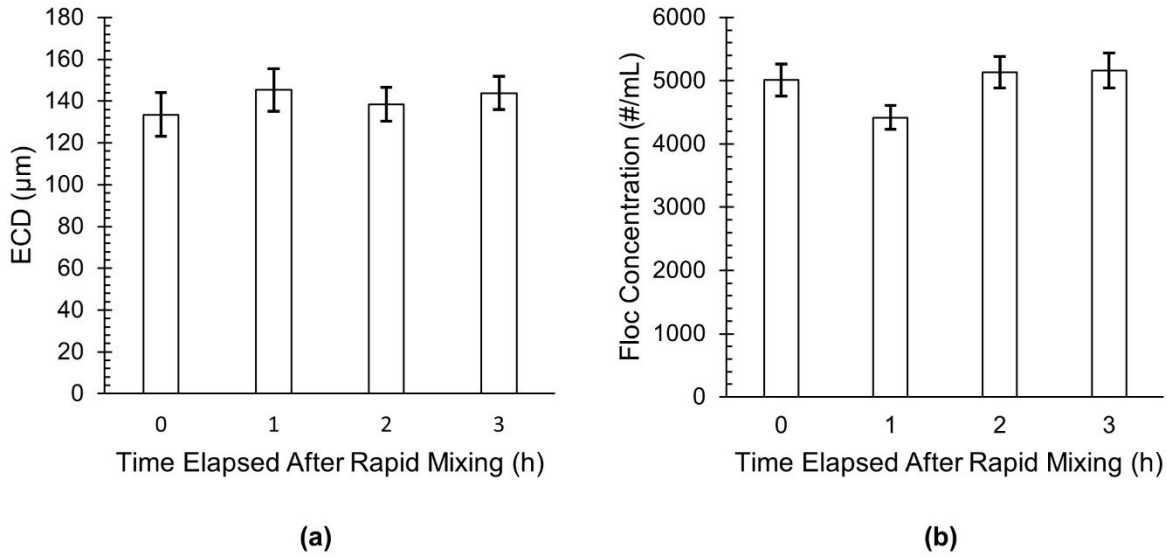

Fig. S7. Kinetic assessment of floc properties in batch reactor system with continuous-stirring at G=200 s^{-1}: **(a)** ECD; **(b)** Floc Concentration.

S.7. Supplemental References

1 H. Yang, N. J. D. Graham, W. Wang, M. Liu and W. Yu, Evaluating and improving the reliability of the UV-persulfate method for the determination of TOC/DOC in surface waters, *Water Res.*, 2021, **196**, 116918.
2 S. K. Maeng, T. C. Timmes and H.-C. Kim, Characteristics of flocs formed by polymer-only coagulation in water treatment and their impacts on the performance of downstream membrane separation, *Environ. Technol.*, 2017, **38**, 2601–2610.
3 J. P. Gonzalez-Galvis and R. M. Narbaitz, Large batch bench-scale dissolved air flotation system (LB-DAF) for drinking water treatability tests, *Environ. Sci. Water Res. Technol.*, 2020, **6**, 1004–1017.
4 J. P. Gonzalez-Galvis and R. M. Narbaitz, Large batch bench-scale dissolved air flotation system for simulating full-scale turbidity removal, *Environ. Technol.*, 2022, **43**, 1791–1804.
5 J. Wang, S. Pan and D. Luo, Characterization of cake layer structure on the microfiltration membrane permeability by iron pre-coagulation, *J. Environ. Sci.*, 2013, **25**, 308–315.
6 J. K. Edzwald and J. E. Tobiason, Enhanced coagulation: US requirements and a broader view, *Water Sci. Technol.*, 1999, **40**, 63–70.
7 H.-C. Kim and B. A. Dempsey, Membrane fouling due to alginate, SMP, EfOM, humic acid, and NOM, *J. Membr. Sci.*, 2013, **428**, 190–197.
8 R. H. Myers, D. C. Montgomery and C. M. Anderson-Cook, *Response Surface Methodology: Process and Product Optimization Using Designed Experiments*, Wiley, Hoboken, NJ, USA, 4th edn., 2016.
9 T. Li, Z. Zhu, D. Wang, C. Yao and H. Tang, Characterization of floc size, strength and structure under various coagulation mechanisms, *Powder Technol.*, 2006, **168**, 104–110.
10 N. Tambo, Physical characteristics of flocs—I. The floc density function and aluminium floc, *Water Res.*, 1979, **13**, 409–419.
11 K. Konieczny, D. Sąkol, J. Płonka, M. Rajca and M. Bodzek, Coagulation—ultrafiltration system for river water treatment, *Desalination*, 2009, **240**, 151–159.
12 A. Amirtharajah and K. M. Mills, Rapid-mix design for mechanisms of alum coagulation, *J. AWWA*, 1982, **74**, 210–216.
13 G. A. Edwards and A. Amirtharajah, Removing color caused by humic acids, *J. AWWA*, 1985, **77**, 50–57.
14 T. R. Hundt and C. R. O'Melia, Aluminum-fulvic acid interactions: mechanisms and applications, *J. AWWA*, 1988, **80**, 176–186.
15 R. V. Lenth, Quick and easy analysis of unreplicated factorials, *Technometrics*, 1989, **31**, 469–473.
16 D. C. Montgomery, *Design and Analysis of Experiments*, Wiley, Hoboken, NJ, USA, 10th edn., 2020.
17 J. C. Crittenden, R. R. Trussell, D. W. Hand, K. J. Howe and G. Tchobanoglous, *Water treatment: Principles and design*, McGraw-Hill, New York, NY, 3rd edn., 2012.